

INFLUENCE OF THE THICKNESS OF THE COMPRESSION HEAD ON THE FRACTURE OF REINFORCED CONCRETE T-BEAMS

Luiz Carlos de Almeida¹ & Gonzalo Ruiz²

¹ Faculdade de Engenharia Civil, Arquitetura e Urbanismo, Universidade Estadual de Campinas
Avenida Albert Einstein, 951
13083-853 Campinas, Brasil
E-mail: almeida@fec.unicamp.br

² E.T.S. de Ingenieros de Caminos, Canales y Puertos, Universidad de Castilla-La Mancha
Avda. Camilo José Cela s/n
13071 Ciudad Real, España
Correo-e: Gonzalo.Ruiz@uclm.es

ABSTRACT

The experimental program reported in this paper was planned to investigate the influence of the thickness of the compression head on the fracture of reinforced concrete T-beams. Particularly, we wanted to corroborate numerical predictions by Ruiz and Carmona (G. Ruiz and J.R. Carmona, *Mater. & Struct.* 39, pp. 343-352, 2006) indicating that such effect is analogous to the effect of the size on the fracture process, i.e. the strength of the beam should vary differently than expected according to traditional mechanics. Besides, in the case of T-beams, the initiation of the crack propagation through the head should also generate a secondary load-peak. To do that we chose scaled T-beams made out of a micro-concrete whose head varied in width from the limit case of the T becoming a rectangle to having a head-thickness equal in length to the beam depth. The micro-concrete mechanical and fracture properties as well as the properties of the steel re-bars and of the interface between the two materials were all obtained from independent tests. The experimental results demonstrate that the cited numerical predictions were correct, since we get a shape-effect curve for the beam strength that resembles variations due to changes in the size. Besides, the beginning of the propagation of the crack through the beam head provokes a secondary load-peak, although it is milder than that predicted numerically.

RESUMEN

El programa experimental que presentamos en este artículo se diseñó para investigar la influencia del espesor de la cabeza de compresión en la fractura de vigas en forma de T de hormigón armado. En particular, queríamos corroborar predicciones numéricas debidas a Ruiz y Carmona (G. Ruiz y J.R. Carmona and D. Cendón, *Mater. & Struct.* 39, pp. 343-352, 2006) que indicaban que dicho efecto es análogo al efecto del tamaño en el proceso de fractura, y así la resistencia de la viga debería variar de modo diferente a lo esperado de acuerdo con la teoría de estructuras tradicional. Además, en el caso de vigas en T la propagación de la fisura del alma a la cabeza debería generar un pico secundario en el registro de la carga. Para ello escogimos vigas en T a escala hechas de un micro-hormigón. El ancho de la cabeza de la viga variaba desde el ancho del alma, en cuyo caso tenemos una sección rectangular como caso límite de una sección en T, hasta un ancho igual al canto de la viga. Las propiedades mecánicas y en fractura del micro-hormigón, las propiedades de las barras de acero y de la intercara entre acero y hormigón se obtuvieron por medio de ensayos independientes. Los resultados experimentales demuestran que las predicciones numéricas citadas eran correctas, ya que la curva que representa el efecto de la forma recuerda las variaciones debidas al efecto del tamaño. Además, el comienzo de la propagación de la grieta a través de la cabeza de la viga en T provoca un pico secundario en la carga, aunque es más suave que el que se predecía numéricamente.

KEYWORDS: Fracture of structural concrete, cohesive models, shape effect, size effect.

1. INTRODUCTION

Various experiments on lightly reinforced beams [1, 2] were based on the idea that minimally reinforced beams are brittle structures susceptible to theoretical analysis by fracture mechanics. These experimental programs showed that brittle collapse of lightly reinforced beams is size dependent, suggesting that the failure is due to fracture processes in concrete. Specifically, Heddal and Kroon [3] considered the bond-slip properties of the

reinforcement and around that they substantially influence the response of the beam. Ruiz et al. [4] made a set of tests that disclosed the influence of several parameters— size, steel ratio, steel yield strength and bond-slip— on the fracture behavior. In addition, they made a complete material characterization by direct testing that made objective numerical modeling possible [5, 6]. However there were still some points to study. On the one hand, most of the works approaching collapse of brittle beams by fracture mechanics have been done on

rectangular beams. Only Ozcebe et al. [7] used a technological approach to study the failure of T beams and Ruiz and Carmona [6] used rectangular beams and one type of T-beams to study the influence of the shape of the crack propagation. On the other hand, Ruiz et al. [8] showed theoretically the existence of a secondary peak in the load record due to the beginning of the propagation of the crack though the head of the beam. With the help of a numerical model they also showed that the crack zone develops as if a T-beam was a larger rectangular beam, which manifests itself in a sort of shape effect. This shape effect is analogous to the effect of the size of the beam, since the load peak increases less than predicted by standard theory of structures as we thicken the head of the beam. Such phenomena had not been observed experimentally and this is why we felt the need of planning and performing an experimental program covering such topics. To do that we chose scaled T-beams made out of a micro-concrete whose head varied in width from the limit case of the T becoming a rectangle to having a head-thickness equal in length to the beam depth. All the beams were made out of the same materials —micro-concrete and steel bars— whose properties remained constant throughout the program. All of the beams had the same number of re-bars arranged in the same way.

The article is structured as follows. A brief overview of the experimental program is given in Section 2. The materials and specimens are described in Section 3. Section 4 summarizes the experimental procedures. The experimental results are presented a discussed in Section 5. Finally, in Section 6 some conclusions are extracted.

2. OVERVIEW OF THE EXPERIMENTAL PROGRAM

The experimental program was intended to study the influence of the shape of the cross-section on the evolution of the fracture process of reinforced beams as they are loaded. We chose scaled T-beams made out of a micro-concrete whose head varied in width from the limit case of the T becoming a rectangle to having a head-thickness equal in length to the beam depth. In addition, the program had to provide material characterization to allow a complete interpretation of the test results that could be useful for future investigations. Finally, the behavior of the laboratory beams should be representative of the behavior of the beams of ordinary size made of ordinary concrete.

Regarding the scale of the specimens, Hillerborg's brittleness number was used as comparison parameter. As a first approximation, two geometrically similar structures will display a similar fracture behavior if their brittleness numbers are equal [3, 6]. β_H is defined as:

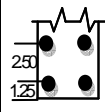
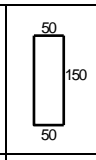
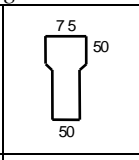
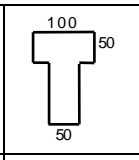
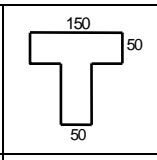
$$\beta_H = \frac{D}{l_{ch}}, \quad \text{where} \quad l_{ch} = \frac{E_c G_F}{f_t^2} \quad (1)$$

where D is the depth of the beam and l_{ch} is the Hillerborg's characteristic length; E_c is the elastic modulus, G_F the fracture energy and f_t the tensile strength. According to this, a relatively brittle micro-concrete was selected with a characteristic length of approximately

77 mm. Since the characteristic length of ordinary concrete is 300 mm on average, laboratory beams 150-mm in depth are expected to simulate the behavior of ordinary concrete beams 450 mm in depth, which is considered reasonable size for the study.

Table 1 sketches the dimensions of the rectangular and T beams chosen, the arrangements of the reinforced bars and names of the specimens for this experimental program.

Table 1 – Rectangular and T cross-section dimensions.

				
	R4-1	TP4-1	TM4-1	TG4-1
	R4-2	TP4-2	TM4-2	TG4-2

Standard characterization and control tests were performed to determine the compressive strength, the tensile strength, the elastic modulus and the fracture energy of the micro-concrete. Likewise the mechanical parameters of the re-bars and the properties of the steel-to-concrete interface were also determined in Laboratory tests.

3. MATERIALS AND SPECIMENS

3.1. Micro-concrete

A single micro-concrete was used throughout the experimentation, made with a lime stone aggregate of 5 mm maximum size that follows the corresponding Fuller curve, and Portland cement 52.5 (ASTM type 1). The mix proportions by weight were 3.0:0.46:1 (aggregate:water:cement). The Abrams cone slump was measured immediately before casting, the average value being 6.5 cm. All the specimens were cast in steel molds, vibrated by a vibrating table, wrap-cured for 24 hours, desmolded, and stored for 5 weeks, until they were tested, in a moist chamber at 20 °C and 98% relative humidity. Table 2 shows the characteristics mechanical parameters of the micro-concrete determined in various characterization and control tests.

Table 2 – Micro-concrete characteristics.

f_c MPa	f_t MPa	E_c GPa	G_F N/m	l_{ch} mm	β_H
52.6	4.6	25.5	64.6	77	1.9

3.2. Steel and Pull-out tests

For the beam dimensions selected, and the desired steel ratios, the diameter of the steel bars had to be smaller than that of standard rebar, so commercial wires with a nominal diameter of 3.0 mm were used to achieve the desired reinforced configuration for different specimens.

Figure 1 shows the stress-strain curve corresponding to the wires used to reinforce the beams. The elastic mod-

ulus is 205 GPa, the standard yield strength for a strain of 0.2% is 765 MPa, and the ultimate strain is 0.6%.

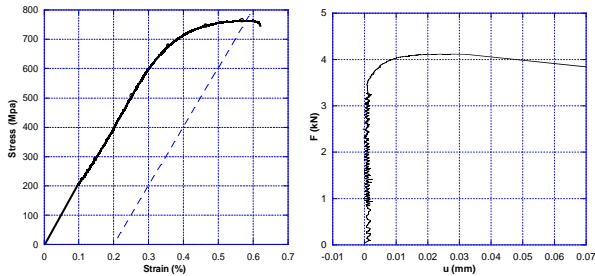


Fig. 1 Stress-strain curve and pull-out test results for wires.

Pull-out specimens consisting of prisms $50 \times 50 \times 75$ mm with a wire embedded along their longitudinal axis. Figure 1 shows the load-slip curve for a typical pull-out test. The resulting mean bond strength was 6.2 MPa.

3.3. Characterization and control specimens

Cylindrical specimens whose dimensions were 150 mm in length and 75 mm in diameter were cast to determine standard mechanical properties. We made 8 specimens, 4 for compression tests and 4 for splitting tests. Notched plain concrete beams were used to characterize concrete fracture properties. All the beams were 50 mm thick, 75 mm deep and 337.5 mm long. The notch was sawn at the central cross-section to depth of half the total beam depth. We made 4 specimens of this type.

3.4. Reinforced micro-concrete beams

Figure 2 and Table 1 summarize the geometrical characteristics of the reinforced concrete beams. The specimens were cast in metallic molds, with the reinforced wires protruding at the end through holes in the mold walls. The micro-concrete was compacted on a vibrat-ing table.

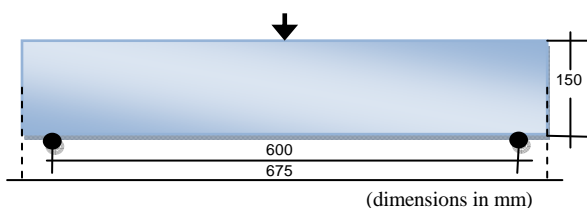


Fig. 2 Beam dimensions and loading conditions.

4. EXPERIMENTAL PROCEDURES

4.1. Characterization and control tests

Compression tests were carried out on 4 cylindrical specimens according to ASTM C39 and C469 except for a reduction in size. The strain was measured over a 50 mm gage length by means of two inductive extensometer placed symmetrically. The tests were run under displacement control, at rate of 0.3 mm/min. Brazilian test were also carried out on 4 cylindrical specimens following the procedures recommended by ASTM C-469. The velocity of displacement of the machine actuator was 0.3 mm/min.

Stable three-point bend tests on notched beams were carried out to obtain the fracture properties of concrete following the procedures devised by Elices, Guinea and Planas [9]. The span was 300 mm. The tests were performed in position control with three linear ramps at different displacement rates: 5 $\mu\text{m}/\text{min}$ during the first 18 min, 25 $\mu\text{m}/\text{min}$ during the following 20 min and 50 $\mu\text{m}/\text{min}$ until the end of test. Figure 3 shows some typical load-displacement curves.

4.2. Reinforced beam tests

The reinforced beams were tested in three-point bending. The first loading ramp was executed in load control until reaching 5 kN in 5 minutes. This loading ramp was fully within the linear response of the beam. According to [6] this type of specimens might show snap-back after the peak-load. So, in order to record that portion of the load-displacement ($P-\delta$) curve, we moved to strain control until the displacement increments were positive again. We were using a clip extensometer attached to the lowermost surface of the beam right below the loading point. The span covered by the clip was 90 mm, and the opening rate was 2 $\mu\text{m}/\text{min}$. The control was successful in almost all of the beams tested. Regrettably, in two of them, namely the beams labeled as R41 and T41, the nucleation of shear cracks out of the zone covered by the clip gage made the machine to lose the control of the tests, which provoked the immediate collapse of the beams. The third, fourth and fifth ramps were performed in position control at 25 $\mu\text{m}/\text{min}$ during 30 min, 125 $\mu\text{m}/\text{min}$ during 10 min and 625 $\mu\text{m}/\text{min}$ until the end of the test respectively. Figure 4 shows some typical load-displacement curves.

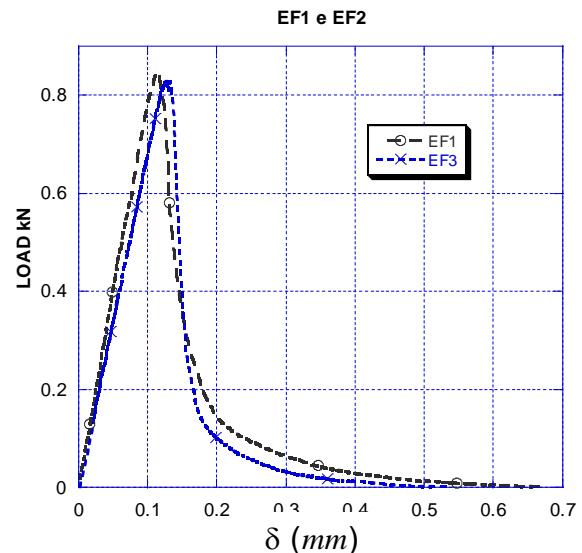


Fig. 3 Curves of load versus load point displacements

5. RESULTS AND DISCUSSION

The main results of the characterization tests are given in Table 2. The Figure 3 shows that the curves of load versus load-point displacement of the stable three-point tests on notched beams area very similar to each other,

which demonstrates the high level of control achieved during the tests.

The experimental P- δ curves for the reinforced beams are shown in Figure 4a. As it is well known, the boundary conditions at the point where the actuator applies the load may generate small variations in the global flexibility of the beam. Consequently, in order to facilitate the comparison between similar beams, the initial slope of the curves is corrected to its theoretical value stemming from Strength of Materials.

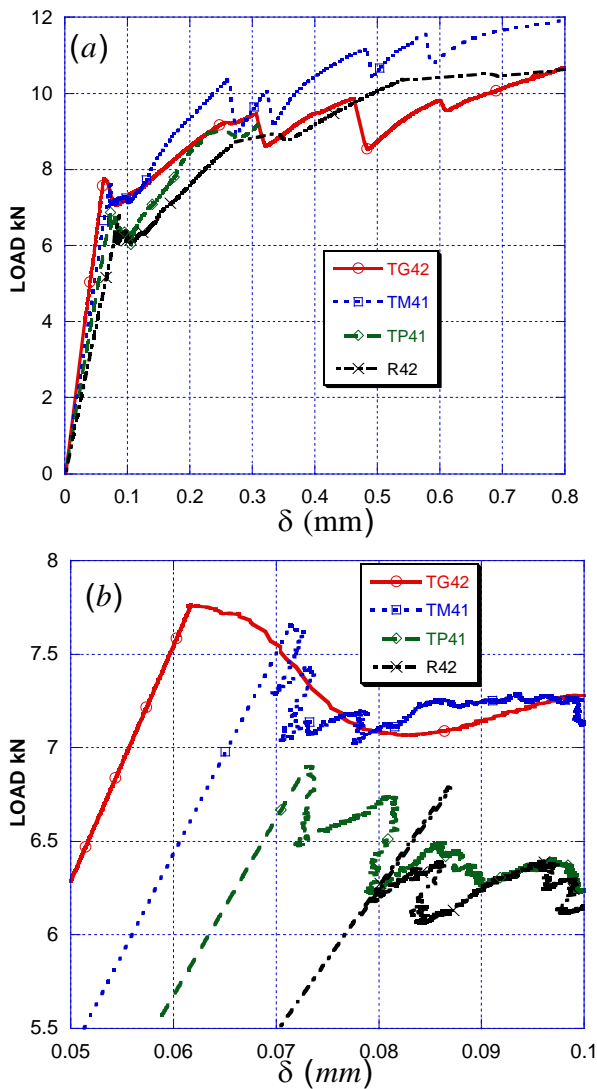


Fig. 4 Load versus load point displacements curves of the beams TG42, TM41, TP41 and R42; and detail of the first load peaks.

Figure 4b shows that after the peak the displacement snaps back while the beam loses resistance, except for the beam TG42. The load transfer between the concrete and the reinforcement enables the beam to recover and generates a U-shaped stretch in the P- δ curve. Fig. 5 shows a zoom of that stretch for the beam TM41. It catches some peaks that correspond to the crack passing through the two layers of reinforcing bars. Right after then, the beam stiffens and the load goes up again. In that ramp-up it is possible to identify a mild hump in the curve that corresponds to the beginning of the propaga-

tion through the head of the beam (Fig. 4a). Soon after that the generation of shear cracks produces a saw-like stretch in the P- δ curve. Each drop in that stretch corresponds to the initiation and sudden growth of a shear crack, which is evidenced by a snap-back in the CMOD record. As the beams are sufficiently reinforced, the ultimate load is higher than the first peak that corresponds to the cracking load.

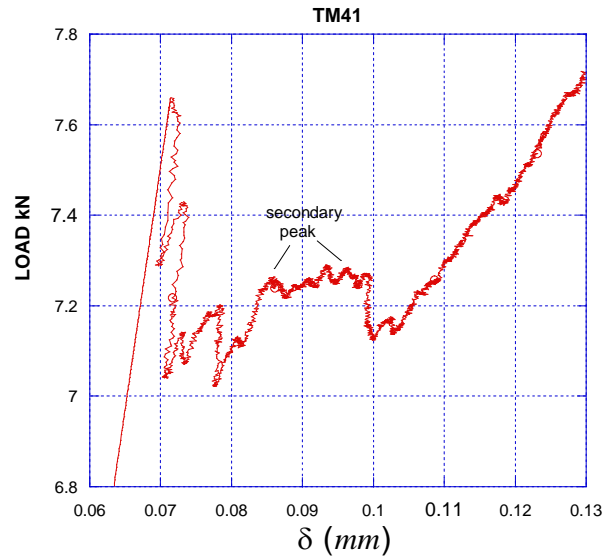


Fig. 5 Detail of the secondary peaks in the load displacement curves of the beam TM41.

Some additional insights on the role of the shape of the cross-section on the strength of the T-beams can be inferred from Fig. 6. The x-axis correspond to the ratio D_{eq}/l_{ch} , where D_{eq} is the equivalent depth of a T-section, which we define as the depth of the rectangular beam that would withstand the same maximum load according to Strength of Materials and making the hypothesis that concrete does not resist tension; l_{ch} is the characteristic length defined in Eq. (1). The y-axis correspond to the ratio P_{max}/P_{nt} , where P_{max} is the maximum load withstood by the T-beams; P_{nt} is the maximum load for the same T-beam obtained according to Strength of Materials plus the no-tension hypothesis.

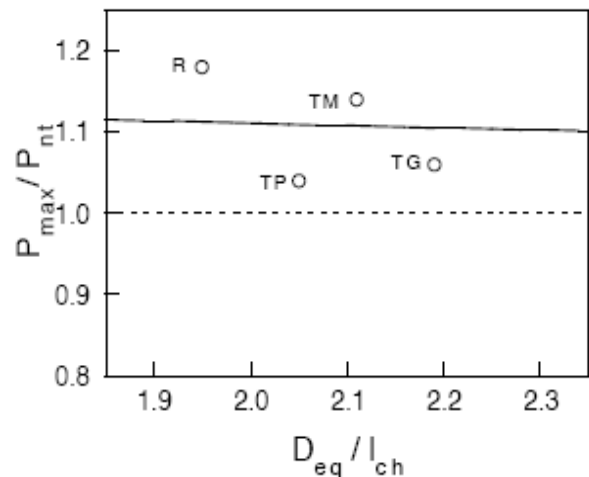


Fig. 6 Effect of the head-thickness.

The points represent the experimental values for P_{\max}/P_{nt} , whereas the solid curve are the numerical loads obtained with the model in [8]. The curve in Fig. 6 reflects the variation of the maximum load (expressed by the non-dimensional ratio P_{\max}/P_{nt}) withstood the T-beams as the width of the head increases (the thickening of the head is represented by the non-dimensional equivalent depth D_{eq}/l_{ch}). The effect of the shape of the cross-section is clear and very similar to what we obtain when it is the size that increases: the ratio P_{\max}/P_{nt} diminishes as the head thickens and tends to be 1 in the limit case of a T-beam whose head width is infinite. The experimental values manifest that there is a slight decrease in the non-dimensional load and validate the existence of the shape effect, i.e. the load peak increase for the T-beams as the head thickens is lower than expected according to traditional mechanics.

6. CONCLUSIONS

This paper presents recent experimental results in T-beams made out of a micro-concrete whose head varied in width from the limit case of the T becoming a rectangle to having a head-thickness equal in length to the beam depth. All the beams were made out of the same materials —micro-concrete and steel bars— whose properties remained constant throughout the program. All of the beams had the same number of re-bars arranged in the same way. The tests were performed so that that fracture process was stable by controlling the strain in the lowermost surface of the beam. The following conclusions can be draw from the study:

- The load-displacement curve shows that there is some hyper-strength attributable to the propagation of the crack through the head of the beam.
- The load-peak increase for the T-beams as the head thickens is lower than expected according to traditional mechanics, and thus this experimental program validates the existence of a *shape effect*.

ACKNOWLEDGMENTS

The authors gratefully acknowledge mobility grants provided by CAPES-Brazil and MEC-Spain and funding from MEC through grant MAT2006-09105.

REFERENCES

- [1] Bosco C., Carpinteri A., Debernardi P.G., Fracture of reinforced concrete: Scale effect and snap-back instability, *Engineering Fracture Mechanics* 35(4-5): 228-236, 1990.
- [2] Carpinteri A., Ed., Minimum Reinforcement in Concrete Members (Number 24 in ESIS Publications. Elsevier, London), 1999.
- [3] Ruiz G., Elices M., Planas J., Experimental study of fracture of lightly reinforced concrete beams, *Materials and Structures* 31 683-691, 1998.
- [4] Ruiz G., Influencia del tamaño y de la adherencia en la armadura mínima de vigas en flexión, (GHEO-IECA, Madrid), 1998.
- [5] Ruiz G., Propagation of a cohesive crack crossing a reinforcement layer, *International Journal of Fracture* 111: 265-282, 2001.
- [6] Ruiz G., Carmona R. J., Experimental study on the influence of the shape of the cross-section and the rebar arrangement on the fracture of LRC beams, *Materials and Structures* 39:343-352, 2006.
- [7] Ozebe G., Ersoy U., Takut T., Minimum flexural reinforcement for T-beams made of high strength, *Canadian Journal of Civil Engineering* 25(5), 1999.
- [8] Ruiz G., Carmona JR., Cendón D.A., Propagation of a cohesive crack through adherent reinforcement layers, *Computer Methods in Applied Mechanics and Engineering* 195 – 7237 – 7248, 2006.
- [9] Elices M., Guinea G. V., Planas J., Measurement of the fracture energy using three-point bend tests. 1 Influence of experimental procedures, *Materials and Structures* 25, 121-218, 1992.